

THIS IS THE SUBMITTED VERSION.

Published version: <https://doi.org/10.1016/j.postharvbio.2022.111910>

Palumbo, M., Pace, B., Cefola, M., Montesano, F. F., Colelli, G., & Attolico, G. (2022). Non-destructive and contactless estimation of chlorophyll and ammonia contents in packaged fresh-cut rocket leaves by a Computer Vision System. *Postharvest Biology and Technology*, 189, 111910.

1 **Non-destructive and contactless estimation of chlorophyll and ammonia contents in packaged**
2 **fresh-cut rocket leaves by a Computer Vision System**

3

4 **Michela Palumbo^{1ab}, Bernardo Pace^{1a}, Maria Cefola^{a*}, Francesco Fabiano Montesano^c,**
5 **Giancarlo Colelli ^b, Giovanni Attolico ^d**

6

7 ^a Institute of Sciences of Food Production, National Research Council of Italy (CNR), c/o CS-DAT,
8 Via Michele Protano, 71121 Foggia, Italy

9 ^b Department of Science of Agriculture, Food and Environment, University of Foggia, Via Napoli 25,
10 71122 Foggia, Italy

11 ^c Institute of Sciences of Food Production, National Research Council of Italy (CNR), Via Giovanni
12 Amendola 122, 70125 Bari, Italy

13 ^d Institute on Intelligent Industrial Systems and Technologies for Advanced Manufacturing, CNR-
14 National Research Council of Italy Via G. Amendola, 122/O, 70126 Bari, Italy

15

16 * Corresponding Author: phone/fax: +39.0881.630201; email address: maria.cefola@ispa.cnr.it

17

18 ¹ **First Authorship is equally shared**

19

THIS IS THE SUBMITTED VERSION.

Published version: <https://doi.org/10.1016/j.postharvbio.2022.111910>

Palumbo, M., Pace, B., Cefola, M., Montesano, F. F., Colelli, G., & Attolico, G. (2022). Non-destructive and contactless estimation of chlorophyll and ammonia contents in packaged fresh-cut rocket leaves by a Computer Vision System. *Postharvest Biology and Technology*, 189, 111910.

20 **Abstract**

21 Computer Vision Systems (CVS) offer a non-destructive and contactless tool to assign visual quality
22 level to fruit and vegetables and to estimate some of their internal characteristics. The innovative
23 CVS described in this paper exploits the combination of image processing techniques and machine
24 learning models (Random Forests) to solve these kind of problems on unpackaged and packaged
25 rocket leaves. Its performance did not depend on the cultivation system (traditional soil or soilless).
26 The same CVS was able to build effective models for either the classification problem (visual quality
27 level assignment) and the regression problems (estimation of senescence indicators such as
28 chlorophyll and ammonia contents) just by changing the training data. The experiments showed a
29 negligible performance loss on packaged products (Pearson's linear correlation coefficient of 0.84
30 for chlorophyll and 0.91 for ammonia) with respect to unpackaged ones (0.86 for chlorophyll and
31 0.92 for ammonia). The results showed that the CVS (non-destructive and contactless) represents a
32 valid alternative to destructive, expensive and time-consuming analyses in the lab and can be
33 effectively and extensively used along the whole supply chain, even on packaged products that cannot
34 be analyzed using traditional tools.

35

36 **Keywords: contactless quality level assessment, *Diplotaxis tenuifolia* L., image analysis,**
37 **packaged vegetables, senescence indicators prediction**

38

39 **1. Introduction**

40 Rocket is a green leafy vegetable usually marketed and consumed as fresh-cut salad, alone or mixed
41 to other leafy vegetables. It is well known and appreciated for its pleasant bitter taste and for its high
42 content in bioactive compounds, such as vitamins, minerals and antioxidants. The two species
43 commonly sold on the market are *Eruca sativa* and *Diplotaxis tenuifolia* or wild rocket that is known
44 to have longer shelf-life (Mastrandrea et al. 2016).

45 The quality loss during the postharvest storage is mainly due to the yellowing of the leaves strictly
46 related to chlorophyll degradation that therefore is the most common index used to evaluate quality
47 and freshness of this product (Limantara et al. 2015; Cavallo et al. 2017). Generally, as reported by
48 Pace et al. (2019), a 30 % loss of total chlorophyll content is considered the shelf-life limit in rocket
49 leaves.

50 Another important indicator of leaves senescence in fresh-cut rocket is ammonia accumulation in
51 plant tissues, as a consequence of the protein breakdown during early stages of senescence. High
52 concentrations of this component may cause tissue damages with visible senescence effects, that
53 impact on the overall quality evaluation of the product (darkening and browning of detached leaves)
54 (Chibnall, 1939; Mastrandrea et al. 2016; Amodio et al. 2018).

55 Traditional approaches for chlorophyll and ammonia content measurements in leafy vegetables
56 include destructive methods, based on spectrophotometric assay.

57 Even if these approaches for a long time have been considered the standard and most used methods
58 for these determinations, they require specific laboratory equipment and destructive sampling and
59 they are expensive and time consuming.

60 While, for the ammonia analysis, the destructive method is widely applied, for chlorophyll evaluation,

61 modern, handheld and sensor have received a considerable attention in the last decades because of
62 their high accuracy and real time measurement in a non-destructive way directly on field or on
63 minimally processed products.

64 So, many researchers have developed several types of chlorophyll meters (Novichonok et al. 2016),
65 multispectral and hyperspectral sensors (Chen et al. 2010; Li et al. 2014) to detect the spectral
66 reflectance of leaves to assess the total chlorophyll content. Many of these techniques are costly and
67 complex and require the presence of specialized personnel. Among them, the most developed
68 instruments widely used for chlorophyll content measurement are fluorimeters (Ferrante and
69 Maggiore, 2007) and SPAD meters (Ling et al. 2011; Liu et al. 2012; Yuan et al. 2016).

70 All these instruments are simpler, faster and cheaper than chemical analysis and other sensor based
71 approaches, but they need to touch the leaf with a probe to carry out a chlorophyll measurement on a
72 limited area of few mm² of leaf surface. For these drawbacks, their use is not suitable for application
73 into an industrial line and, additionally, the estimation of chlorophyll content is strictly related to the
74 quality of sampling (Cavallo et al. 2017).

75 Recently, in order to reduce these disadvantages, image analysis based on common digital camera
76 has been applied as a low cost instrument for the assessment of chlorophyll content on leafy
77 vegetables, becoming a potential approach for smart agriculture (Mohan and Gupta, 2019) and
78 postharvest quality assessment (Pace et al. 2014, 2015; Cavallo et al. 2017).

79 Machine vision systems have proved to be more robust than area-based instruments as they work at
80 pixel level considering the entire visible surface of the product. Many research works on the use of
81 digital image both during cultivation and postharvest were reported to evaluate total chlorophyll
82 content of leaves of rice (Wang et al. 2013, 2014), soybean (Rigon et al. 2016), corn (Vesali et al.
83 2017), spinach (Agarwal and Gupta, 2018) and rocket leaves (Cavallo et al. 2017; Pace et al. 2019),
84 also through the use of common smartphone cameras that are often associated to high speed processor

85 (Mohan and Gupta, 2019). The success of Computer Vision System (CVS) is due to the possibility
86 of establishing relationships between spectral reflectance indices and chlorophyll absorbance and
87 RGB (red, green and blue) components of an image (Santos do Amaral et al. 2019).
88 Recently, Cavallo et al. (2018) also applied the image analysis technology to packed and unpacked
89 fresh-cut iceberg lettuce to assess the quality levels of the product with similar performances both on
90 packaged and unpacked samples. The main purpose of this study was to achieve a careful selection
91 of the bag area where the product was visible with a quality suitable for image analysis. All images
92 acquired on packed samples were segmented using a Convolutional Neural Network (CNN),
93 identifying and selecting only pixels belonging to the fresh-cut lettuce without interferences of the
94 affected regions of bag. These Authors recorded a performance loss of only about 3 % due to the
95 presence of packaging (accuracy of 83 % on packed product instead of 86 % on unpacked one),
96 showing the power of image analysis in monitoring the quality level of fresh-cut vegetables. The
97 CNN segmentation method was able to separate the graphical elements and the regions affected by
98 lighting artefacts from the product inside the commercial bag, demonstrating its real applicability on
99 an industrial line, regardless the presence of the packaging. The proposed approach has been the only
100 CVS application in the quality level assessment of vegetables through the packaging and, certainly,
101 further investigations are needed to confirm and implement this emerging technology for a continuous
102 check of the quality of fresh-cut products along the whole supply chain.
103 Few application regarding the use of CVS for the detection of ammonia content in leafy vegetables,
104 are reported. In Pace et al. (2014), CVS was applied on whole and fresh-cut lettuce to give a non-
105 destructive evaluation of this chemical parameter often used as a senescence indicator in several leafy
106 vegetables (Cefola and Pace, 2015; Tudela et al. 2013). Starting from these considerations, the aims
107 of the research reported in this paper were to verify and assess the capability of the non-destructive
108 and contactless CVS in: i) assessing the visual quality changes during postharvest storage of fresh-

109 cut rocket leaves; ii) estimating some internal characteristics (chlorophyll and ammonia contents) of
110 fresh-cut rocket leaves; iii) working through the packaging without significant performance loss due
111 to the identification of the regions where the product is properly visible. This region identification, in
112 the experiments described in this paper, has been accomplished using a simplified techniques based
113 on data-driven image processing without the need of training a Convolutional Neural Network
114 (CNN).

115

116 **2. Materials and Methods**

117 *2.1. Plant material and experimental setup*

118 Rocket leaves (*Diplotaxis tenuifolia* L. cv Dallas) were cultivated at the same time in soil or soilless
119 cultivation systems at the CNR-ISPA experimental farm La Noria (CNR-ISPA) located in Mola di
120 Bari (in the South of Italy). Harvests were performed at 55, 70 and 110 days and at 60, 110 and 145
121 days after sowing for soilless and soil system, respectively.

122 At each harvest time, fresh-cut rocket leaves, separated per cultivation system were provided to the
123 laboratory for image analysis by CVS and postharvest quality determinations. Thus, fresh-cut leaves
124 were selected to avoid samples with defects and mechanical damages and packed in open PP bags
125 (dimensions 50 x 30 cm, Orved, Musile di Piave (VE), Italy) of about 600 g each one. In detail, 13
126 bags (replicates) were prepared for samples cultivated on soil system, while 10 bags for rocket leaves
127 cultivated on soilless system. Then, all samples were stored at 10 °C (the storage temperature
128 commonly used in the supply chain) for 16 and 18 days for soilless and soil system, respectively.

129

130 *2.2. Sensory visual quality attribution during cold storage of rocket leaves.*

131 During storage, samples were taken and observed to attribute the visual quality level (QL) according
132 to the scale reported by Palumbo et al. (2021).

133 In detail, at each sampling day, an amount of sample was taken from each PP bag and evaluated by
134 a group of 5 researchers using the 5 to 1 rating scale cited above, where 5 = very good (very fresh, no
135 signs of yellowing, bright, dark and uniform green, no defects), 4 = good (fresh, slight signs of
136 yellowing, light green, slight loss of texture), 3 = fair (slight wilting, moderate signs of yellowing,
137 slight discoloration, minor defects, loss of texture), 2 = poor (wilting, evident yellowing,
138 discoloration, severe loss of texture), 1 = very poor (unacceptable quality due to decay, severe wilting
139 and yellowing, complete loss of texture and other evident defects). A score of 3 was considered to be
140 the limit of marketability, while a score of 2 represented the limit of edibility.

141 Then, images of packaged and unpackaged fresh-cut rocket leaves were acquired by CVS and the
142 quality of the same samples was evaluated through destructive conventional methods as detailed
143 below.

144

145 *2.3. Colour analysis by colorimeter, total chlorophyll content, ammonia content, and electrolyte* 146 *leakage*

147 The CIELAB colour parameters (L^* , a^* and b^*) were detected, for each replicate, on 3 random points
148 on the surface of 10 rocket leaves using a colorimeter (CR400, Konica Minolta, Osaka, Japan). The
149 instrument was calibrated with a standard reference having values of L^* , a^* and b^* corresponding to
150 97.44, 0.10 and 2.04, respectively. Then, the colour parameter of Hue angle (h°) was calculated from
151 primary L^* , a^* and b^* readings according the equation below:

152

$$153 \quad h^\circ = \tan^{-1} \frac{b^*}{a^*} \quad (1)$$

154

155 The total chlorophyll content was measured according to the spectrophotometric method reported by
156 Cefola and Pace (2015). Five grams of rocket leaves were chopped and extracted in acetone/water

157 (80:20 v/v) with a homogenizer (T-25 digital ULTRA-TURRAX® - IKA, Staufen, Germany) and
158 then centrifuged at 6440 xg for 5 min. To remove all pigments, the extraction was repeated 5 times
159 (10 mL per times) and extracts were combined. The absorbance was read immediately after the
160 extraction procedure on extracts proper diluted using a spectrophotometer (UV-1800, Shimadzu,
161 Kyoto, Japan) at three wavelengths, at 663.2 nm, 646.8 nm, and 470 nm. Total chlorophyll content
162 was expressed as $mg\ g^{-1}$ of fresh weight using the equation reported by Wellburn (1994).

163 Ammonia content was evaluated according to Fadda et al. (2016). Chopped rocket leaves (5 g) were
164 homogenized for 2 min in 20 mL of distilled water on an ice bath, and then centrifuged for 5 min at
165 6440 xg at 4 °C. Then, the supernatant extract (0.5 mL), was mixed with 5 mL of nitroprusside reagent
166 (phenol and hypochlorite in alkali reaction mixture) and heated at 37 °C for 20 min. The color
167 development after incubation, was determined with the spectrophotometer (reading the absorbance at
168 635 nm). The content of NH_4^+ was expressed as $\mu g\ NH_4^+\ g^{-1}$ of fresh weight, using ammonium sulfate
169 as standard (0–10 $\mu g\ mL^{-1}$, $R^2 = 0.99$).

170 The electrolyte leakage was determined following the method reported by Palumbo et al. (2021). In
171 detail, about 2.5 g of rocket leaves disks obtained using a cork borer (\varnothing 8 mm) were placed in plastic
172 tubes and immersed in 25 mL of distilled water. After 30 min of storage at 10 °C, the conductivity of
173 the solution was measured using a conductivity meter (Cond. 51+ - XS Instruments, Carpi, Italy).
174 Then, the tubes with samples and solution were frozen at – 20 °C and, after 48 h, the conductivity
175 was detected after thawing and considered as total conductivity. Electrolyte leakage was calculated
176 as the percentage ratio of initial over total conductivity.

177

178 2.4. *Image analysis by computer vision system*

179 At each sampling day, a sample of about 60 g of product was taken from each replicate and was
180 placed inside a 20 x 25 cm PP bags (Cartonpack Rutigliano, Italy). Three images of the packaged

181 product were acquired by randomly shuffling the rocket in the bag before each acquisition: this
 182 procedure generated three different images from each packaged sample to increase the amount of
 183 observed surface and the variability of visual appearance considered by the CVS. Then, the same
 184 product was extracted from the bag and three images were acquired by randomly shuffling and
 185 stacking the leaves before each acquisition. In this way, for each replicate the CVS acquired 6 images:
 186 3 of the packaged product and 3 of the unpackaged product. Example of the six images acquired from
 187 a single sample are shown in Figure 1.

188 Therefore, 78 images were available at each time for samples coming from soil system (6 images for
 189 each of the 13 replicates) and 60 images for samples coming from the soilless system (6 images for
 190 each of the 10 replicates).

191 The final dataset was composed by 429 and 450 image from soil and soilless cultivation respectively
 192 after all three harvest date. In Table 1 the number of acquisitions conducted for each harvest time on
 193 packaged and unpackaged products are reported. The complete collection was therefore composed
 194 by 879 images for each packaged or unpackaged product. We choose to not distinguish images
 195 coming from different harvests: therefore, the final image dataset was composed by 207 images for
 196 the quality level 5 and by 168 images for each quality level from 4 to 1. These data are reported in
 197 the Table 1.

198

199 **Table 1.** Composition of the dataset of images with respect to harvests (H1, H2 and H3), and quality
 200 levels (QL).

	<i>Soil</i>							<i>Soilless</i>						
	Replicates	QL					Total	Replicates	QL					Total
		5	4	3	2	1			5	4	3	2	1	
<i>H 1</i>	13	15	15	15	15	15	75	10	15	15	15	15	15	75
		15	15	15	15	15	75		15	15	15	15	15	75
		9	9	9	9	9	45		-	-	-	-	-	-
<i>H 2</i>	13	15	15	15	15	15	75	10	15	15	15	15	15	75

		15	15	15	15	15	75		15	15	15	15	15	75
		9	9	9	9	9	45		-	-	-	-	-	-
H 3	13	15	-	-	-	-	15	10	15	15	15	15	15	75
		15	-	-	-	-	15		15	15	15	15	15	75
		9	-	-	-	-	9		-	-	-	-	-	-
		117	78	78	78	78	429		90	90	90	90	90	450

201

202 *2.5. Image processing steps by Computer Vision System*

203 The following paragraphs describe all the processing steps used by the CVS. All the software was
 204 developed using Matlab 2019a (Mathworks Inc.). A flowchart of the processing steps (whose
 205 sequence is slightly different for packaged and unpackaged products) along with their effects on the
 206 images, is shown in Figure 2.

207

208 *2.5.1. Acquisition of calibrated color images*

209 To acquire calibrated color images, color changes due to environment conditions (lighting, geometry,
 210 sensor instability) were evaluated and reduced to the minimum. Images were acquired using the set-
 211 up reported in (Pace et al. 2015, 2017; Cavallo et al. 2017, 2018) using a 3CCD (with a dedicated
 212 Charged Coupled Device for each color channel) digital camera (JAI CV-M9GE) having a resolution
 213 of 1024 x 768 pixels. The imaged area is about 32 x 24 cm. A 3CCD sensor has been used to avoid
 214 the artifacts introduced by the demosaicing methods required to record color information using a
 215 single CCD. The optical axis of the LinosMeVis 12 mm lens system was perpendicular to the black
 216 background. Two DC power suppliers delivered current to eight halogen lamps, placed along two
 217 rows at the two sides of the imaged area and oriented at a 45° angle with respect to the optical axis.
 218 All the images were saved using the uncompressed TIFF format to avoid the artifacts introduced by
 219 compression algorithms.

220

221 *2.5.2. Color-chart processing and foreground segmentation*

222 A small X-Rite color-chart with 24 patches of known colors was placed into the scene to measure
223 color variations due to environmental conditions and sensor characteristics by comparing the
224 expected numerical values released by the manufacturer with the ones acquired by the camera. The
225 color-chart was automatically detected regardless of its position and orientation (Cavallo et al. 2017).
226 All the colors in the color-chart were used to estimate the linear transformation used for color
227 correction.

228 Image processing worked only on the part of each image belonging to the product at hand
229 (foreground), while the background was discarded. The CVS automatically separated foreground and
230 background without any human intervention: two thresholds were derived from the analysis of the
231 whole image in the HSV color space as described in (Cavallo et al. 2017). This segmentation
232 identified the region belonging to the product as a whole and did not separate its different parts neither
233 discarded any region of leaves. It was designed to be conservative, that is to discard all the background
234 pixels even at the cost of removing some marginal borders of the product. It removed also background
235 area inside the stack of leaves as long as part of leaves too dark (for example for self-shadowing of
236 the product) to provide meaningful color information.

237 *2.5.3. Color correction*

238 Color correction needs to be effective (able to provide consistent color measurements) and efficient
239 (computationally simple enough to be suitable for real applications along the supply chain). The linear
240 correction model proved to be the best trade-off between effectiveness and computational complexity
241 and it was used in the experiments (Palumbo et al. 2021).

242 Let it be $[r_e^i \ g_e^i \ b_e^i]^T$ and $[r_m^i \ g_m^i \ b_m^i]^T$ the expected and the measured RGB values respectively for
243 the i -th patch $i=1, \dots, 24$. A linear correction (LC) model, a 3×3 matrix, was evaluated to reduce the
244 distance between the expected and the measured values on the color chart:

245

246

$$\begin{bmatrix} r_c \\ g_c \\ b_c \end{bmatrix} = \begin{pmatrix} m_{11} & m_{12} & m_{13} \\ m_{21} & m_{22} & m_{23} \\ m_{31} & m_{32} & m_{33} \end{pmatrix} \begin{bmatrix} r_m \\ g_m \\ b_m \end{bmatrix}$$

247

where $\begin{bmatrix} r_c \\ g_c \\ b_c \end{bmatrix}$ are the colors corrected using the matrix whose elements were evaluated using a least-

248

square approach and all the patches of the color-chart. The same matrix was therefore used to correct

249

all the foreground pixels of the image.

250

The linear transformation was different for each image (it was evaluated from the color-chart

251

appearance in each specific image) to adapt to the specific conditions of each acquisition. The linear

252

correction requires 73 ms.

253

254

2.5.4. Artefact elimination from packaging

255

The unpredictable relative orientation of the surface of the bag with respect to light can easily generate

256

artefacts such as reflections. In those regions, the camera cannot measure the true colors of the product

257

at hand: therefore, those pixels are useless to estimate internal components or to assign visual quality.

258

Before feature extraction and classification or regression, those areas must be removed from each

259

image and only the regions where the product is visible with meaningful colors must be maintained.

260

The flowchart in the Figure 2 shows the placement of the artefact elimination step inside the

261

processing chain and its effects on the image. To identify the useless regions, the image converted in

262

the HSV (Hue-Saturation-Value) color space was considered. In this space, it is possible to exploit

263

the characteristics of artefacts that are mainly colorless and much brighter than the product. Two data

264

driven thresholds were automatically extracted on the Hue (thresh_h) and on the Value (thresh_v)

265

components of the image using the Otsu algorithm: pixels whose hue was greater than thresh_h and

266

whose value was lower than thresh_v were considered as belonging to product and maintained for the

267 following processing. The Figure 2 shows an example of the obtained result. The region left for
268 further processing is significantly reduced: a conservative choice was made also in this case, by
269 preferring to discard more pixels of product instead of leaving saturated pixels in the image. The
270 resulting valid area proved to be large enough to allow the feature extraction and the classification
271 and regression phases.

272

273 2.5.5. Features extraction

274 On the base of previous experiences, the device independent and perceptually uniform CIE $L^*a^*b^*$
275 color space was chosen to accomplish color analysis. Because the L^* component is fragile, being too
276 sensible to not uniform illumination levels across the scene, the complete histogram in the $a^* b^*$ plane
277 of the foreground pixels was used as feature set for both classification and regression. The color
278 histogram represents the number of occurrences of each color, that is of each (a^*, b^*) pair, in all the
279 foreground pixels: it therefore represents a property of the whole observed product. The continuous
280 (a^*, b^*) plane was discretized using 30 bins for each axis (a^* and b^*): therefore, the complete
281 histogram was a matrix with 900 elements. This representation is more detailed than statistical
282 measures such as mean, median or standard deviation: it describes completely the palette of colors
283 present in the scene and their relative relevance. The hypotheses were that such information was able
284 to represent the appearance of new colors due to senescence, in according with changes in content of
285 internal components such as chlorophyll and ammonia. To avoid any human intervention in the
286 identification of proper color features, the complete matrix containing all the values of the bins of this
287 histogram was reshaped as a vector and passed to the classification phase. The use of a quite large
288 vector with 900 elements was feasible because the ensemble method used for classification and
289 regression can sample for each tree a subset of even a quite large set of features: this approach
290 automatically figures out their best use while keeping reasonable the computational complexity. Even

291 if it is not possible to identify few specific colors suitable to discriminate product quality and internal
292 contents of chlorophyll and ammonia, the ensemble of trees exploits a reasonably large subset of the
293 provided features, that is (a^*, b^*) pairs, to achieve the desired goals.

294

295 2.5.6. *Image analysis*

296 To assign the visual quality to a sample is an example of a classification problem: the model needs to
297 assign a value out of a finite set of choices (in this case a quality level from 5 to 1 as described above).

298 To estimate the chlorophyll and ammonia contents is instead an example of a regression problem: the
299 model needs to estimate a real number in a continuous interval. In both cases, a supervised learning
300 approach was followed: a model was chosen and its parameters were fixed on the base of the analysis
301 of available samples. Each sample was composed by a set of features (the whole histogram in the a -
302 b plane of the CIE $L^*a^*b^*$ color space as described in the paragraph above) and the expected answers:
303 an integer value (in the set from 1 to 5) defining the visual quality level (used for classification) and
304 two real values for chlorophyll and ammonia respectively (used for regression).

305 A Random Forest model was used to accomplish both classification and regression (Breiman, 1996,
306 2001). In case of classification, a model was trained to assign the QL to the product. In case of
307 regression, two different models were trained to estimate the chlorophyll content and the ammonia
308 content of the product respectively. In all the cases, the models shared the same architecture and differ
309 for the free parameters that were fixed for the specific task. The values of the cells of the histogram
310 in the $a^* b^*$ plane (of the CIE $L^*a^*b^*$ color space) of each image provided the vocabulary of features
311 used for training the models. The approach, for training each tree, randomly sampled the available
312 training data (to select the training examples) and randomly selected a set of features (in this case
313 randomly selecting which values of the histogram to use to build the tree at hand). Each tree of the
314 forest was allowed to have a maximum of 10 branches. Due to the limited number of samples, a 10-

315 fold cross validation approach was used: that means to divide the available data into 10 groups (folds),
316 each having approximately the same number of elements. The partitions were made with
317 stratification: therefore, each fold approximated the same distribution of the whole training set.
318 According to the 10-folds validation strategy, at each iteration of the process the training was done
319 10 times: at each round, a different fold was separated for testing the results while the other nine folds
320 were used for training. The average of the results obtained in the ten rounds estimated the performance
321 of the method at each iteration.

322 To increase the stability of results, 10 iterations were run for each task (classification for visual
323 quality, regression for chlorophyll estimation, regression for ammonia estimation): the best result of
324 the ten iterations and the average of their results were stored. The best value was very similar to the
325 average, proving that the randomness of the choice of training samples and of features for each tree
326 did not affect significantly the performance of the resulting model.

327 *2.5.6.1 Classification*

328 Accuracy was used as a quick indicator of the performance of classification in the results' section
329 but, to provide a complete description of the obtained results, the confusion matrices were also stored:
330 in fact, they express all the information needed to describe the behavior of the method. The provided
331 confusion matrices and accuracy values represent the average of the values over these 10 different
332 iterations, each corresponding to a new random stratified partition of training data into 10 folds. That
333 increases the significance of the obtained results by making less relevant the effects of chance in
334 sampling training data and features. In spite of the significative number of trees in the resulting forest
335 (200 trees were allowed for each forest) the increase in accuracy provided by their combination did
336 not require high computational costs. The code, written in Matlab without any specific optimization,
337 required about 2 minutes for building the Random Forest model and about 10 milliseconds to apply
338 the model to a new sample and to classify it.

339

340 *2.5.6.2 Regression*

341 Mean square error (MSE) and Pearson's correlation coefficient between the estimated and the true
342 values measured in the lab were used to quantify the performance of regression. To increase the
343 robustness of performance measures, the 10-fold cross-validation regression was repeated 10 times
344 (iterations). The best values and the average values are provided for both chlorophyll and ammonia
345 estimation. In spite of the significative number of trees in the resulting forest (200 trees were allowed
346 for each forest) the increase in accuracy provided by their combination does not require high
347 computational costs. The code, written in Matlab without any specific optimization, requires about 6
348 minutes for building the Random Forest model and about 2 milliseconds to apply the model to a new
349 sample and to estimate the desired parameter.

350

351 *2.6. Statistical analysis*

352 A one-way ANOVA was performed to study the relationship between the most important quality
353 parameters (total chlorophyll content, ammonia content, hue angle and electrolyte leakage) and the
354 QLs during the rocket leaves cold storage (10 °C) with the aim of identifying the physical and
355 chemical parameters able to classify in an objective and consistent way the QLs of rocket leaves.
356 The mean values were separated using the Student-Newman-Keuls (SNK) test and Statgraphics
357 Centurion (version 18.1.12, Warrenton, Virginia, USA) was used for statistical analyses.
358 Partial least squares regression (PLSR) was run using the software The Unscrambler X.

359

360 **3. Results and Discussion**

361 *3.1. Changes in quality parameters during storage of fresh-cut rocket leaves*

362 During storage the change in the sensory QL from 5 to 1 was mainly due to the yellowness of rocket
363 leaves, as showed in Figure 3.

364

365 **Table 2.** Hue angle, total chlorophyll content, ammonia content and electrolyte leakage in fresh-cut
366 rocket leaves cultivated on different cultivation systems (soil, soilless or all samples) and stored at 10
367 °C at each quality level

<i>Parameter</i>	<i>Quality Level</i>					<i>P-value</i>
	5 <i>very good</i>	4 <i>good</i>	3* <i>fair</i>	2 <i>poor</i>	1 <i>very poor</i>	
<i>Soil system</i>						
Hue angle (h°)	125.6 a	124.7 a	121.3 b	118.1 c	114.4 d	****
Total chlorophyll content (mg g^{-1})	0.9 a	0.7 b	0.6 c	0.5 d	0.4 e	****
Ammonia content ($\mu\text{g NH}_4^+ \text{g}^{-1}$)	7.3 c	3.1 c	6.8 c	89.7 b	184.3 a	****
Electrolyte leakage (%)	12.7 e	21.0 d	26.2 c	30.8 b	40.7 a	****
<i>Soilless system</i>						
Hue angle (h°)	126.8 a	125.5 b	123 c	119.6 d	116.8 e	****
Total chlorophyll content (mg g^{-1})	0.7 a	0.7 a	0.5 b	0.4 c	0.4 c	****
Ammonia content ($\mu\text{g NH}_4^+ \text{g}^{-1}$)	4.3 c	2.9 c	9.9 c	38.5 b	80.1 a	****
Electrolyte leakage (%)	18.9 c	20.3 c	23.5 b	27.2 a	28.0 a	****
<i>All samples (soil and soilless)</i>						
Hue angle (h°)	126.1 a	125.2 b	122.2 c	118.8 d	115.6 e	****
Total chlorophyll content (mg g^{-1})	0.8 a	0.7 b	0.6 c	0.5 d	0.4 e	****
Ammonia content ($\mu\text{g NH}_4^+ \text{g}^{-1}$)	3.0 c	6.0 c	8.4 c	67.8 b	133.7 a	****
Electrolyte leakage (%)	15.9 e	20.6 d	24.6 c	28.8 b	34.1 a	****

*: limit of marketability.

For each parameter the mean values followed by different letters are significantly different (P -value < 0.05) according to Student-Newman-Keuls (SNK) test.Significance: **** = significant at P -value ≤ 0.0001

Quality level: 5=very good; 4= good; 3=fair; 2=poor; 1=very poor

368

369 Considering the quality parameters determined during the rocket leaves storage, a significant
370 separation of the visual QL was obtained by colour analysis (Table 2). In detail, for samples cultivated
371 on soil system the h° colour parameter separated the leaves very good (QL5) and good (QL4) from

372 fair (QL3), poor (QL2) and very poor (QL1) ones, showing a decrease of about 8.9 % from QL5 to
373 QL1. In soilless cultivation system, all the QLs of rocket leaves were well separated by h° . Its value
374 decreased from 126.8 ± 0.9 in QL5 to 116.8 ± 3.2 in waste samples (QL1). The same QL separation
375 was obtained by h° value when all samples (soilless and soil) were considered (Table 2). Similar
376 results were reported by Mastrandrea et al. (2016) in which h° values decreased from 124 to 115 in
377 rocket leaves stored at 10 °C. Hue angle is considered a qualitative attribute of colour, according to
378 which colours are defined as greenish, reddish, yellowish and so on. Higher h° represents a lower
379 yellow trait in the product (Pathare et al. 2013). In the present study, h° values decreased during the
380 storage, indicating a gradual yellowing of rocket leaves from QL5 to QL1.

381 Moreover, a significant relationship was also found between decreasing visual QL and total
382 chlorophyll and ammonia content, which can be considered objective markers of quality loss for
383 rocket leaves (Table 2). In particular, for samples produced on soil system, total chlorophyll content
384 was able to discriminate all the QLs, recording a significant decrease from QL5 (0.9 mg g^{-1}) to QL1
385 (0.4 mg g^{-1}). The chlorophyll content allowed to have the same QL discrimination when the samples
386 from soil and soilless system were joined (Table 2). For samples cultivated on soilless system, the
387 chlorophyll content at harvest was 24.6 % lower than that measured in samples cultivated on soil
388 system. Many research works proved the influence of pre-harvest factors on the postharvest quality
389 of vegetables and the cultivation system is one of them (Frezza et al. 2010; Elia and Colelli, 2009).
390 In this study, the soilless system produced a lower (-24 %) chlorophyll content at harvest (QL5) with
391 respect to the soil one, reducing the intensity of the green colour of the leaves. On the contrary, at the
392 end of storage (QL1), the samples cultivated on the two different system, showed similar values
393 (about 0.4 mg g^{-1}) with a reduction of about 50 % for the samples from soil system. Additionally, the
394 chlorophyll content in samples grown on soilless system proved to discriminate the very good (QL5)
395 and good (QL4) rocket leaves from fair (QL3), in which a decrease of 16.3 % was recorded;

396 furthermore, marketable samples (QL3) were well discriminated from edible (QL2) and waste (QL1)
397 ones. The chlorophyll degradation during the postharvest storage is strictly related to the senescence
398 of the product. Chlorophyll plays an important role as primary photosynthetic pigment and it is
399 responsible of the specific colour of the plant leaf. It is commonly used as parameter of maturity,
400 quality and freshness of green leafy vegetables because it is involved into leaves senescence process
401 (Limantara et al. 2015; Cavallo et al. 2017). At harvest, rocket leaves are dark or bright green in
402 colour, but during senescence changes into yellow, with a general loss of visual quality. It is well
403 known that one of the factors associated with the loss of freshness and marketability in green leafy
404 vegetables, such as rocket leaves, is an increase of yellowing associated to chlorophyll degradation
405 (Cefola et al. 2010; Watkins, 2006). This process involves many enzymatic reactions in chloroplasts
406 and vacuoles and, particularly, leaves yellowing is strictly related to the activity of chlorophyllase, an
407 enzyme that catalyzes the Type I chlorophyll breakdown in vegetables (Matile et al. 1999; Shi et al.
408 2016; Li et al. 2017). Many authors suggested that ethylene production in damaged tissues (such as
409 in fresh-cut products) is responsible for the chlorophyll loss because it causes an increase of the
410 chlorophyllase activity (Yamauchi and Watada, 1991). Moreover, some studies about chlorophyll
411 loss in fresh-cut produces reported evidence of the breakdown induced by oxygen radical oxidation
412 of the chlorophyll. Indeed, chlorophyll breakdown take place also when a physiological stress occurs
413 on the tissues, such as the mechanical stress induced by cutting (Toivonen and Brummel, 2008;
414 Torales et al. 2020). This chlorophyll breakdown related to the action of oxidative enzymes is
415 classified as Type II and it can be controlled by antioxidant treatments, as reported by Cefola and
416 Pace (2015) who used oxalic acid treatments to control the chlorophyll oxidation on rocket leaves
417 during storage at 8 °C. In the present study, the chlorophyll decrease, resulting in yellowing of leaves
418 at the end of storage at 10 °C, was probably due to both the types of breakdown (Type I and Type II)

419 above mentioned, in accordance with the evolution of the activity of the enzymes related to the
420 chlorophyll degradation observed by Torales et al. 2020 on fresh-cut rocket leaves during cold stored.
421 The same QL discrimination was observed in the case of ammonia content for both cultivation
422 systems and for all samples, recording a rapid increase from QL3 to QL1 (Table 2). In particular, this
423 parameter well separated the marketable samples (QL5, QL4 and QL3) from the non-marketable ones
424 (QL2 and QL1); moreover, even the waste samples (QL1) were well discriminated from the edible
425 ones (QL2). At QL1 samples cultivated on soil system showed 56.3 % higher ammonia content than
426 that grown on soilless system. Similar results were reported by Pace et al. (2014) who identify in the
427 ammonia content a good classifier for whole and fresh-cut iceberg lettuce, separating the acceptable
428 product (ranged from QL5 to QL3) from the edible (QL2) and waste (QL1) ones. Ammonia
429 accumulation in plant tissues as a consequence of protein catabolism is another aspect associated with
430 the leaf senescence in leafy vegetables. High concentrations of this compound may cause tissue
431 damages with visible senescence effects, that impact on the overall quality evaluation of the product.
432 Chibnall (1939) first reported that ammonia accumulation was the cause of darkening and browning
433 of detached leaves during postharvest, also later demonstrated by Cantwell et al. (2010) on spinach
434 leaves and Mastrandrea et al. (2016) on rocket leaves. Generally, leafy vegetables under stressful
435 condition showed a reduction in the glutamine synthetase activity, an enzyme that leads to the
436 ammonia reintegration during protein synthesis (Chandra et al. 2006). So, large amount of ammonia
437 is accumulated into cells because of its toxicity, but this cause tissue damages (Toivonen, 1997). In
438 addition, ammonia accumulation occurs very often in closed systems, such as a package, where may
439 reach high levels. Indeed, in minimally processed products, deteriorative processes like proteolysis
440 are enhanced by injuries occurred during handling steps, especially in highly active products (such as
441 green leafy vegetables) (Wang et al. 2004; Cefola et al. 2010), and by the activity of phenylalanine
442 ammonia-lyase, that cause lignification of tissues, releasing ammonia (Joy, 1988). Moreover, Yang

443 et al. 1982 demonstrated that also ethylene biosynthesis process from methionine produces little
444 amount of ammonia. Many authors demonstrated that ammonia is a good indicator of rocket
445 senescence as of other leafy vegetables and its accumulation could be the cause of the darkening
446 process linked to leaves senescence (Chibnall,1939). Mastrandrea et al. (2016), and subsequently
447 confirmed by Amodio et al. (2018), reported high correlations ($R^2 > 0.98$) between changes in
448 ammonia content and hue angle variations (that correspond to yellowing) in rocket leaves stored at
449 10 °C. As for the detection of ammonia content in leafy vegetables by CVS, an application of this
450 non-invasive methodology on whole and fresh-cut lettuce was reported by Pace et al. (2014) to give
451 a non-destructive evaluation of this chemical parameter particularly useful for the objective
452 evaluation of food quality. In particular, the Authors studied the correlation coefficient between the
453 quality levels and the ammonia content of products using the percent brown area of images acquired
454 by CVS to build predictive models.

455 The electrolyte leakage was closely related to the quality and shelf life of fresh-cut produce and it is
456 a physical parameter commonly used to measure the intensity of oxidative damages to cell
457 membranes due to reactive oxygen species development in fresh-cut tissues (Kou et al. 2014). So,
458 higher values in electrolytic leakage indicate higher physiological stress of leaves tissues. In this
459 research, electrolyte leakage significantly increased in rocket leaves obtained by soil system (from
460 12.7 ± 4.2 % in QL5 to 40.7 ± 7.6 % in QL1), well discriminating all the five QLs (Table 2). The
461 same QL separation was observed considering all samples, with a significant increase of electrolyte
462 leakage from the QL5 (15.9 ± 4.9 %) to QL1 (34.1 ± 9.1 %). On the contrary, this parameter in rocket
463 leaves cultivated on soilless system proved to significantly discriminate very good (QL5) and good
464 (QL4) from fair (QL3), recording an increase of 24.3 %. Moreover, in this cultivation system, the
465 QL3 samples were well separated from edible (QL2) and waste ones (QL1). Similar results were
466 reported by Palumbo et al. (2021) on rocket leaves cultivated under soilless cultivation system and

467 stored at 10 °C, in which this parameter was able to discriminate the marketable samples (QL5 and
 468 QL4) from the fair (QL3) and the waste (QL2 and QL1) ones. In the present research work, the
 469 percentage increase of electrolyte leakage along the different QLs in rocket leaves grown on soil
 470 system was higher (220.5 %) than that detected on samples cultivated under soilless system (48.1 %),
 471 pointing out that the last cultivation system was probably more efficient in terms of reduction of
 472 induced oxidative stresses on cell membranes (Bonasia et al. 2017).

473

474 3.2. Non-destructive quality evaluation of packed and unpacked rocket leaves by CVS

475 Computer Vision System was applied to estimate the visual QL of packaged fresh-cut rocket and to
 476 predict the total chlorophyll and the ammonia content in packaged and unpacked rocket leaves.

477 Regarding the first task, table 3, 4 and 5 show the results obtained considering three different cases:

478 i) to separate non-marketable product (QL 1 and 2) from marketable product (QL from 3 to 5); ii) to
 479 increase the resolution to separate edible but not marketable product (QL 2) from waste (QL 1); iii)
 480 to further increase the resolution to separate also the limit of marketable product (QL 3).

481 In all these case, the CVS was able to operate through the packaging with negligible loss of accuracy.

482 Moreover, the increase in class separation (from Table 3 to Table 5) showed a reduction in accuracy

483 on soilless samples (and therefore when all the samples were considered). Instead, the accuracy

484 remained at high level for samples coming from the soil system.

485

486 **Table 3.** Confusion matrix obtained separating 2 class (QL 1-2, QL 3-4-5).

QL	<i>Unpacked</i>			<i>Packed</i>			
	QL		Accuracy (r)	QL		Accuracy (r)	
	1-2	3-4-5		1-2	3-4-5		
<i>All samples</i>	1-2	273	63	0.899	281	55	0.907
	3-4-5	26	517		27	516	

<i>Soil</i>	1-2	152	4	0.981	141	15	0.947
	3-4-5	3	270		7	266	
<i>Soilless</i>	1-2	147	33	0.893	146	34	0.891
	3-4-5	15	255		15	255	

487

488

489

490

491

492

493

494

495 **Table 4.** Confusion matrix obtained separating 3 class (QL 1, QL2, QL 3-4-5).

	QL	<i>Unpacked</i>			<i>Accuracy</i> (r)	<i>Packed</i>			<i>Accuracy</i> (r)
		QL				QL			
		1	2	3-4-5		1	2	3-4-5	
<i>All samples</i>	1	116	34	18	0.831	122	37	9	0.826
	2	22	86	60		28	79	61	
	3-4-5	1	13	528		0	18	525	
<i>Soil</i>	1	72	6	0	0.954	69	9	0	0.905
	2	6	68	4		9	53	16	
	3-4-5	0	4	269		0	6	267	
<i>Soilless</i>	1	74	13	3	0.829	69	18	3	0.826
	2	14	40	36		10	43	37	
	3-4-5	0	11	259		0	10	260	

496

497 **Table 5.** Confusion matrix obtained separating 4 class (QL 1, QL2, QL 3, QL 4-5).

QL	<i>Unpacked</i>			<i>Packed</i>		
	QL			QL		

		1	2	3	4-5	Accuracy (r)	1	2	3	4-5	Accuracy (r)
<i>All samples</i>	1	119	42	6	2	0.738	121	42	3	1	0.724
	2	24	99	16	29		28	101	11	27	
	3	1	23	72	72		0	29	57	81	
	4-5	0	1	14	360		0	7	12	356	
<i>Soil</i>	1	71	7	0	0	0.909	68	10	0	0	0.86
	2	6	68	4	0		10	59	7	2	
	3	0	4	62	12		0	9	55	14	
	4-5	0	0	6	189		0	1	7	188	
<i>Soilless</i>	1	74	15	1	0	0.703	70	20	0	0	0.673
	2	14	51	15	10		12	52	8	18	
	3	0	19	22	49		1	16	15	58	
	4-5	0	1	9	170		0	6	8	166	

498

499 The results obtained by the CVS in estimating the chlorophyll and ammonia contents of all the
500 samples and of items cultivated on soil or soilless are reported in Table 6. For each case, the Pearson's
501 correlation coefficient and MSE are shown. For each value, the best result and the average of results
502 obtained over 10 repetitions are reported. The tables compare the results obtained on unpackaged
503 product with the ones obtained on packaged product. Figure 4 plots the values estimated by the CVS
504 against the values measured in the lab for ammonia on unpackaged (A) and packaged (B) products
505 and chlorophyll content on unpackaged (C) and packaged (D) samples. In figure 4 all the samples are
506 drawn, regardless their cultivation system. The negligible differences between the best values and the
507 average ones show that the randomness used in the construction of the model does not affect
508 significantly the performance of the method. The small differences between the values related to
509 unpackaged and packaged products confirm that the method is able to operate also through the bag.

510

511 **Table 6.** Mean Squared Error (MSE) and Pearson's correlation coefficient (r) measured to predict by
512 CVS total chlorophyll and ammonia content of unpackaged and packaged fresh-cut rocket.

Samples	<i>Total Chlorophyll</i>				<i>Ammonia Content</i>				
	Unpackaged		Packaged		Unpackaged		Packaged		
	Best	Average	Best	Average	Best	Average	Best	Average	
<i>Soil and Soiless</i>	MSE	77.62	78.65	90.23	91.41	575.1	588.7	643.0	656.3
	r	0.87	0.87	0.84	0.84	0.92	0.92	0.91	0.91
<i>Soil</i>	MSE	69.55	70.45	72.20	74.05	746.9	782.1	872.5	908.0
	r	0.90	0.90	0.90	0.89	0.94	0.94	0.93	0.92
<i>Soiless</i>	MSE	66.52	68.42	83.81	84.68	284.3	289.0	314.6	326.0
	r	0.83	0.83	0.78	0.78	0.87	0.86	0.85	0.84

513

514 *3.3. Estimation of visual quality level of packed fresh-cut rocket using as predictors total chlorophyll*
 515 *and ammonia measured by conventional methods or by CVS.*

516 Three PLS models were built to predict the visual QL using as predictors the total chlorophyll and
 517 the ammonia contents obtained by destructive methods (Model I), CVS trough packaging (Model II)
 518 and CVS without packaging (Model III). The points in the graphics, for each model, represent the
 519 average of the data for each QL for Soil and Soiless systems.

520 The Figure 5 shows the biplot and the comparison between predicted and reference values for
 521 calibration (blu) and validation (red) step for three model: Model I is related to data measured in the
 522 laboratory, Model II uses data estimated by the CVS on packaged products, Model III uses data
 523 estimated by the CVS on unpackaged products. In the graphics, the two factors are a linear
 524 combination of both the predictors (chlorophyll and ammonia) even if Factor 1 and Factor 2 weight
 525 more the ammonia and the total chlorophyll contents respectively. The predictors estimated non-
 526 destructively and contactless by the CVS (Model II and Model III) provide better performances in
 527 predicting the visual QL than the ones measured by the destructive analysis in the laboratory, in both
 528 calibration and validation. This is probably due to the wider area of product observed by the CVS,

529 larger than the amount of product used by the destructive methods. It is also evident that the difference
530 between Model II (related to the CVS applied to packaged product) and Model III (related to the CVS
531 applied to unpackaged product) is negligible. These results further confirm the ability of the CVS to
532 evaluate the product also through the bag, even working only on the regions of the image that provide
533 meaningful colour information about the product's surface.

534

535 **4. Conclusion**

536 The research described in this paper aims to develop and validate a CVS that can assess the quality
537 changes of fresh-cut rocket leaves and estimate their total chlorophyll and ammonia contents during
538 postharvest storage, in a non-destructive and contactless way. All the quality parameters determined
539 by destructive conventional methods during the fresh-cut rocket leaves storage were significant to
540 separate the visual QLs and, among them, total chlorophyll and ammonia contents were very useful
541 marker parameters in the assessment of all the considered QLs.

542 The CVS was able to operate even through the packaging material, enabling these controls along the
543 whole supply chain.

544 The proposed CVS is based on the use of calibrated colour images and on the proper combination of
545 image processing techniques and machine learning models. It was able to solve the classification
546 problem (assigning the visual quality level) and the regression problems (estimating the chlorophyll
547 and ammonia contents) using the same supervised learning methodology (Random Forest) applied to
548 proper training data. The results proved that the system can be a valid alternative to conventional
549 destructive measures, offering the advantage of being non-destructive, contactless, fast and cheap.
550 Moreover, experiments showed that the loss in performance due to the observation of product through
551 the packaging is negligible.

THIS IS THE SUBMITTED VERSION.

Published version: <https://doi.org/10.1016/j.postharvbio.2022.111910>

Palumbo, M., Pace, B., Cefola, M., Montesano, F. F., Colelli, G., & Attolico, G. (2022). Non-destructive and contactless estimation of chlorophyll and ammonia contents in packaged fresh-cut rocket leaves by a Computer Vision System. *Postharvest Biology and Technology*, 189, 111910.

552 The PLS models built to predict the visual QL using as predictors total chlorophyll and ammonia
553 content further confirmed the ability of the CVS to operate also through the packaging. The predictors
554 estimated non-destructively and contactless by the CVS (Model II and Model III) outperformed the
555 ones measured by destructive analysis in the laboratory in predicting the visual QL in both calibration
556 and validation.

557 Therefore, the developed CVS represents a cheap, fast, non-destructive and contactless tool to
558 monitor packaged and unpackaged products along the whole supply chain.

559

560 **Acknowledgments**

561 The authors thank Michele Attolico of STIIMA-CNR and Arturo Argentieri of ISASI-CNR for the
562 technical support to the configuration of the experimental set-up, Massimo Franchi and Mariella
563 Quarto of CNR-ISPA for the technical and administrative support, respectively.

564 This research was funded by the project Prin 2017 “SUS&LOW-Sustaining low-impact practices in
565 horticulture through non-destructive approach to provide more information on fresh produce history
566 and quality” (grant number: 201785Z5H9) from the Italian Ministry of Education University.

567

568

569

570

571

572 **References**

573 Agarwal, A., Gupta, S.D., 2018. Assessment of spinach seedling health status and chlorophyll content
574 by multivariate data analysis and multiple linear regression of leaf image features. *Comput. Electron.
575 Agric.* 152, 281-289. <https://doi.org/10.1016/j.compag.2018.06.048>

THIS IS THE SUBMITTED VERSION.

Published version: <https://doi.org/10.1016/j.postharvbio.2022.111910>

Palumbo, M., Pace, B., Cefola, M., Montesano, F. F., Colelli, G., & Attolico, G. (2022). Non-destructive and contactless estimation of chlorophyll and ammonia contents in packaged fresh-cut rocket leaves by a Computer Vision System. *Postharvest Biology and Technology*, 189, 111910.

576

577 Amodio, M.L., Colelli, G., Cantwell, M.I., 2018. Ammonia accumulation in plant tissues: a
578 potentially useful indicator of postharvest physiological stress. *Acta Hortic.* 1194, 1511–
579 1518. doi:10.17660/actahortic.2018.1194.211

580

581 Bonasia, A., Lazzizzera, C., Elia, A., Conversa, G., 2017. Nutritional, biophysical and physiological
582 characteristics of wild rocket genotypes as affected by soilless cultivation system, salinity level of
583 nutrient solution and growing period. *Front. Plant Sci.* 8,
584 300. <https://doi.org/10.3389/fpls.2017.00300>

585

586 Breiman, L., 1996. Bagging predictors. *Mach. Learn.* 24, 123–140

587

588 Breiman, L., 2001. Random forests. *Mach. Learn.* 45, 5–32

589

590 Cantwell, M., Hong, G., Nie, X., 2009. Using tissue ammonia and fermentative volatile
591 concentrations as indicators of beneficial and stressful modified atmospheres for leafy and floral
592 vegetables, in: X International Controlled and Modified Atmosphere Research Conference. 876 (pp.
593 165-172). 10.17660/ActaHortic.2010.876.20

594

595 Cavallo, D.P., Cefola, M., Pace, B., Logrieco, A.F., Attolico, G., 2018. Non-destructive automatic
596 quality evaluation of fresh-cut iceberg lettuce through packaging material. *J. Food Eng.* 223, 46-52.
597 <https://doi.org/10.1016/j.jfoodeng.2017.11.042>

598

THIS IS THE SUBMITTED VERSION.

Published version: <https://doi.org/10.1016/j.postharvbio.2022.111910>

Palumbo, M., Pace, B., Cefola, M., Montesano, F. F., Colelli, G., & Attolico, G. (2022). Non-destructive and contactless estimation of chlorophyll and ammonia contents in packaged fresh-cut rocket leaves by a Computer Vision System. *Postharvest Biology and Technology*, 189, 111910.

- 599 Cavallo, D.P., Cefola, M., Pace, B., Logrieco, A.F., Attolico, G., 2017. Contactless and non-
600 destructive chlorophyll content prediction by random forest regression: A case study on fresh-cut
601 rocket leaves. *Comput. Electron. Agric.* 140, 303-310. <https://doi.org/10.1016/j.compag.2017.06.012>
602
- 603 Cefola, M., Pace, B., 2015. Application of oxalic acid to preserve the overall quality of rocket and
604 baby spinach leaves during storage. *J. Food Process.* 39(6), 2523-2532. doi:10.1111/jfpp.12502
605
- 606 Cefola, M., Amodio, M.L., Rinaldi, R., Vanadia, S., Colelli, G., 2010. Exposure to 1-
607 methylcyclopropene (1-MCP) delays the effects of ethylene on fresh-cut broccoli raab (*Brassica rapa*
608 L.). *Postharvest Biol. Technol.* 58(1), 29-35. <https://doi.org/10.1016/j.postharvbio.2010.05.001>
609
- 610 Chandra, D., Matsui, T., Suzuki, H., Kosugi, Y., 2006. Postharvest changes in some physiological
611 traits and activities of ammonia-assimilating enzymes in lettuce during storage. *Asian J. Plant Sci.* 5
612 (2), 378–384. <https://doi.org/10.3923/ajps.2006.378.384>.
613
- 614 Chen, P., Haboudane, D., Tremblay, N., Wang, J., Vigneault, P., Li, B., 2010. New spectral indicator
615 assessing the efficiency of crop nitrogen treatment in corn and wheat. *Remote Sens. Environ.* 114(9),
616 1987-1997. <https://doi.org/10.1016/j.rse.2010.04.006>
617
- 618 Chibnall, A.C., 1939. The role of proteins in the respiration of detached leaves, in: Chibnall, A.C.
619 (Ed), *Protein Metabolism in the Plant*. New Haven, CT, USA: Yale University Press, pp. 211–243.
620
- 621 Colelli, G., Elia, A., 2009. I prodotti ortofrutticoli di IV gamma: aspetti fisiologici e tecnologici. *Italus*
622 *Hortus.* 16(1), 55-78.

THIS IS THE SUBMITTED VERSION.

Published version: <https://doi.org/10.1016/j.postharvbio.2022.111910>

Palumbo, M., Pace, B., Cefola, M., Montesano, F. F., Colelli, G., & Attolico, G. (2022). Non-destructive and contactless estimation of chlorophyll and ammonia contents in packaged fresh-cut rocket leaves by a Computer Vision System. *Postharvest Biology and Technology*, 189, 111910.

623

624 Fadda, A., Pace, B., Angioni, A., Barberis, A., Cefola, M., 2016. Suitability for ready-to-eat
625 processing and preservation of six green and red baby leaves cultivars and evaluation of their
626 antioxidant value during storage and after the expiration date. *J. Food Process.* 40(3), 550-558.
627 <https://doi.org/10.1111/jfpp.12634>

628

629 Ferrante, A., Maggiore, T., 2007. Chlorophyll *a* fluorescence measurements to evaluate storage time
630 and temperature of Valeriana leafy vegetables. *Postharvest Biol. Technol.* 45(1), 73-80.
631 <https://doi.org/10.1016/j.postharvbio.2007.02.003>

632

633 Frezza, D., Logegaray, V.R., León, A.P., Harris, M., Chiesa, A., 2009. Rocket (*Eruca sativa* Mill.)
634 quality affected by preharvest and postharvest factors, in: Southeast Asia Symposium on Quality and
635 Safety of Fresh and Fresh-Cut Produce. 875 (pp. 357-364). 10.17660/ActaHortic.2010.875.45

636

637 Joy, K.W., 1988. Ammonia, glutamine, and asparagine: a carbon–nitrogen interface. *Can. J.*
638 *Bot.* 66(10), 2103-2109. <https://doi.org/10.1139/b88-288>

639

640 Kou, L., Yang, T., Luo, Y., Liu, X., Huang, L., Codling, E., 2014. Pre-harvest calcium application
641 increases biomass and delays senescence of broccoli microgreens. *Postharvest Biol. Technol.* 87, 70-
642 78. <https://doi.org/10.1016/j.postharvbio.2013.08.004>

643

644 Li, D., Li, L., Ge, Z., Limwachiranon, J., Ban, Z., Yang, D., Luo, Z., 2017. Effects of hydrogen sulfide
645 on yellowing and energy metabolism in broccoli. *Postharvest Biol. Technol.* 129, 136-142.
646 <https://doi.org/10.1016/j.postharvbio.2017.03.017>

THIS IS THE SUBMITTED VERSION.

Published version: <https://doi.org/10.1016/j.postharvbio.2022.111910>

Palumbo, M., Pace, B., Cefola, M., Montesano, F. F., Colelli, G., & Attolico, G. (2022). Non-destructive and contactless estimation of chlorophyll and ammonia contents in packaged fresh-cut rocket leaves by a Computer Vision System. *Postharvest Biology and Technology*, 189, 111910.

647

648 Li, F., Mistele, B., Hu, Y., Chen, X., Schmidhalter, U., 2014. Reflectance estimation of canopy
649 nitrogen content in winter wheat using optimised hyperspectral spectral indices and partial least
650 squares regression. *Eur. J. Agron.* 52, 198-209. <https://doi.org/10.1016/j.eja.2013.09.006>

651

652 Limantara, L., Dettling, M., Indrawati, R., Brotosudarmo, T.H.P., 2015. Analysis on the chlorophyll
653 content of commercial green leafy vegetables. *Procedia Chem.* 14, 225-231.
654 <https://doi.org/10.1016/j.proche.2015.03.032>

655

656 Ling, Q., Huang, W., Jarvis, P., 2011. Use of a SPAD-502 meter to measure leaf chlorophyll
657 concentration in *Arabidopsis thaliana*. *Photosyn. Res.* 107(2), 209-214.
658 <https://doi.org/10.1007/s11120-010-9606-0>

659

660 Liu, Z.A., Yang, J.P., Yang, Z.C., 2012. Using a chlorophyll meter to estimate tea leaf chlorophyll
661 and nitrogen contents. *J. Soil Sci. Plant Nutr.* 12(2), 339-348. [http://dx.doi.org/10.4067/S0718-](http://dx.doi.org/10.4067/S0718-95162012000200013)
662 [95162012000200013](http://dx.doi.org/10.4067/S0718-95162012000200013)

663

664 Mastrandrea, L., Amodio, M.L., Cantwell, M.I., 2016. Modeling ammonia accumulation and color
665 changes of arugula (*Diplotaxis tenuifolia*) leaves in relation to temperature, storage time and cultivar.
666 *Acta Hortic.* 1141, 275-282. DOI: 10.17660/ActaHortic.2016.1141.34

667

668 Matile, P., Hörtensteiner, S., Thomas, H., 1999. Chlorophyll degradation. *Annu. Rev. Plant*
669 *Biol.*, 50(1), 67-95. <https://doi.org/10.1146/annurev.arplant.50.1.67>

670

THIS IS THE SUBMITTED VERSION.

Published version: <https://doi.org/10.1016/j.postharvbio.2022.111910>

Palumbo, M., Pace, B., Cefola, M., Montesano, F. F., Colelli, G., & Attolico, G. (2022). Non-destructive and contactless estimation of chlorophyll and ammonia contents in packaged fresh-cut rocket leaves by a Computer Vision System. *Postharvest Biology and Technology*, 189, 111910.

671 Mohan, P.J., Gupta, S.D., 2019. Intelligent image analysis for retrieval of leaf chlorophyll content of
672 rice from digital images of smartphone under natural light. *Photosynthetica*. 57(2), 388-398. DOI:
673 10.32615/ps.2019.046

674

675 Novichonok, E.V., Novichonok, A.O., Kurbatova, J.A., Markovskaya, E.F., 2016. Use of the
676 atLEAF+ chlorophyll meter for a nondestructive estimate of chlorophyll content.
677 *Photosynthetica*. 54(1), 130-137. DOI: 10.1007/s11099-015-0172-8

678

679 Pace, B., Cavallo, D.P., Cefola, M., Burbaci, S., Attolico, G., 2019. Colour analysis to predict the
680 total chlorophyll content of rocket leaves, in: VI International Symposium on Applications of
681 Modelling as an Innovative Technology in the Horticultural Supply Chain Model-IT 1311 (pp. 107-
682 112). 10.17660/ActaHortic.2021.1311.14

683

684 Pace, B., Cavallo, D.P., Cefola, M., Attolico, G., 2017. Automatic identification of relevant colors in
685 non-destructive quality evaluation of fresh salad vegetables. *Int. J. of Food Processing Technol.* 4(1),
686 1-5. DOI: <http://dx.doi.org/10.15379/2408-9826.2017.04.01.01>

687

688 Pace, B., Cavallo, D.P., Cefola, M., Colella, R., Attolico, G., 2015. Adaptive self-configuring
689 computer vision system for quality evaluation of fresh-cut radicchio. *Innov. Food Sci. Emerg.*
690 *Technol.* 32, 200-207. <https://doi.org/10.1016/j.ifset.2015.10.001>

691

692 Pace, B., Cefola, M., Da Pelo, P., Renna, F., Attolico, G., 2014. Non-destructive evaluation of quality
693 and ammonia content in whole and fresh-cut lettuce by computer vision system. *Food Res. Int.* 64,
694 647-655. <https://doi.org/10.1016/j.foodres.2014.07.037>

THIS IS THE SUBMITTED VERSION.

Published version: <https://doi.org/10.1016/j.postharvbio.2022.111910>

Palumbo, M., Pace, B., Cefola, M., Montesano, F. F., Colelli, G., & Attolico, G. (2022). Non-destructive and contactless estimation of chlorophyll and ammonia contents in packaged fresh-cut rocket leaves by a Computer Vision System. *Postharvest Biology and Technology*, 189, 111910.

695

696 Palumbo, M., Pace, B., Cefola, M., Montesano, F.F., Serio, F., Colelli, G., Attolico, G., 2021. Self-
697 configuring CVS to discriminate rocket leaves according to cultivation practices and to correctly
698 attribute visual quality level. *Agronomy*, 11(7), 1353. <https://doi.org/10.3390/agronomy11071353>

699

700 Pathare, P.B., Opara, U.L., Al-Said, F.A.J., 2013. Colour measurement and analysis in fresh and
701 processed foods: a review. *Food Bioproc Tech.* 6(1), 36-60. [https://doi.org/10.1007/s11947-012-](https://doi.org/10.1007/s11947-012-0867-9)
702 0867-9

703

704 Rigon, J.P.G., Capuani, S., Fernandes, D.M., Guimarães, T.M., 2016. A novel method for the
705 estimation of soybean chlorophyll content using a smartphone and image analysis. *Photosynthetica*.
706 54(4), 559-566. <https://doi.org/10.1007/s11099-016-0214-x>

707

708 Santos do Amaral, E., Silva, D.V., Dos Anjos, L., Schilling, A.C., Dalmolin, Â.C., Mielke, M.S.,
709 2019. Relationships between reflectance and absorbance chlorophyll indices with RGB (Red, Green,
710 Blue) image components in seedlings of tropical tree species at nursery stage. *New For.* 50(3), 377-
711 388. <https://doi.org/10.1007/s11056-018-9662-4>

712

713 Shi, J., Gao, L., Zuo, J., Wang, Q., Wang, Q., Fan, L., 2016. Exogenous sodium nitroprusside
714 treatment of broccoli florets extends shelf life, enhances antioxidant enzyme activity, and inhibits
715 chlorophyll-degradation. *Postharvest Biol. Technol.* 116, 98-104.
716 <https://doi.org/10.1016/j.postharvbio.2016.01.007>

717

THIS IS THE SUBMITTED VERSION.

Published version: <https://doi.org/10.1016/j.postharvbio.2022.111910>

Palumbo, M., Pace, B., Cefola, M., Montesano, F. F., Colelli, G., & Attolico, G. (2022). Non-destructive and contactless estimation of chlorophyll and ammonia contents in packaged fresh-cut rocket leaves by a Computer Vision System. *Postharvest Biology and Technology*, 189, 111910.

718 Toivonen, P.M., Brummell, D.A., 2008. Biochemical bases of appearance and texture changes in
719 fresh-cut fruit and vegetables. *Postharvest Biol. Technol.* 48(1), 1-14.
720 <https://doi.org/10.1016/j.postharvbio.2007.09.004>

721

722 Torales, A.C., Gutiérrez, D.R., Rodríguez, S.D.C., 2020. Influence of passive and active modified
723 atmosphere packaging on yellowing and chlorophyll degrading enzymes activity in fresh-cut rocket
724 leaves. *Food Packag.* 26, 100569. <https://doi.org/10.1016/j.fpsl.2020.100569>

725

726 Tudela, J.A., Marín, A., Garrido, Y., Cantwell, M., Medina-Martínez, M.S., Gil, M.I., 2013. Off-
727 odour development in modified atmosphere packaged baby spinach is an unresolved
728 problem. *Postharvest Biol. Technol.* 75, 75-85. <https://doi.org/10.1016/j.postharvbio.2012.08.006>

729

730 Vesali, F., Omid, M., Mobli, H., Kaleita, A., 2017. Feasibility of using smart phones to estimate
731 chlorophyll content in corn plants. *Photosynthetica.* 55(4), 603-610. DOI: 10.1007/s11099-016-
732 0677-9

733

734 Wang, Y., Wang, D., Shi, P., Omasa, K., 2014. Estimating rice chlorophyll content and leaf nitrogen
735 concentration with a digital still color camera under natural light. *Plant methods.* 10(1), 1-11.
736 <https://doi.org/10.1186/1746-4811-10-36>

737

738 Wang, Y., Wang, D., Zhang, G., Wang, J., 2013. Estimating nitrogen status of rice using the image
739 segmentation of GR thresholding method. *Field Crops Res.* 149, 33-39.
740 <https://doi.org/10.1016/j.fcr.2013.04.007>

741

THIS IS THE SUBMITTED VERSION.

Published version: <https://doi.org/10.1016/j.postharvbio.2022.111910>

Palumbo, M., Pace, B., Cefola, M., Montesano, F. F., Colelli, G., & Attolico, G. (2022). Non-destructive and contactless estimation of chlorophyll and ammonia contents in packaged fresh-cut rocket leaves by a Computer Vision System. *Postharvest Biology and Technology*, 189, 111910.

742 Wang, Y.T., Yang, C.Y., Chen, Y.T., Lin, Y., Shaw, J.F., 2004. Characterization of senescence-
743 associated proteases in postharvest broccoli florets. *Plant Physiol. Biochem.* 42(7-8), 663-670.
744 <https://doi.org/10.1016/j.plaphy.2004.06.003>

745

746 Watkins, C.B., 2006. The use of 1-methylcyclopropene (1-MCP) on fruits and
747 vegetables. *Biotechnol. Adv.* 24(4), 389-409. <https://doi.org/10.1016/j.biotechadv.2006.01.005>

748

749 Wellburn, A.R., 1994. The spectral determination of chlorophylls a and b, as well as total carotenoids,
750 using various solvents with spectrophotometers of different resolution. *J. Plant Physiol.* 144(3), 307-
751 313. [https://doi.org/10.1016/S0176-1617\(11\)81192-2](https://doi.org/10.1016/S0176-1617(11)81192-2)

752

753 Yamauchi, N., Watada, A.E., 1991. Regulated chlorophyll degradation in spinach leaves during
754 storage. *J. Am. Soc. Hortic. Sci.* 116(1), 58-62. <https://doi.org/10.21273/JASHS.116.1.58>

755

756 Yang, S.F., Adams, D.O., Lizada, C., Yu, Y., Bradford, K.J., Cameron, A.C., Hoffman, N.E., 1982.
757 Mechanism and regulation of ethylene biosynthesis, in: *Plant growth substances*. Springer, Berlin,
758 Heidelberg (pp. 219-229). https://doi.org/10.1007/978-3-642-67720-5_21

759

760 Yuan, Z., Ata-Ul-Karim, S.T., Cao, Q., Lu, Z., Cao, W., Zhu, Y., Liu, X., 2016. Indicators for
761 diagnosing nitrogen status of rice based on chlorophyll meter readings. *Field Crops Res.* 185, 12-20.
762 <https://doi.org/10.1016/j.fcr.2015.10.003>

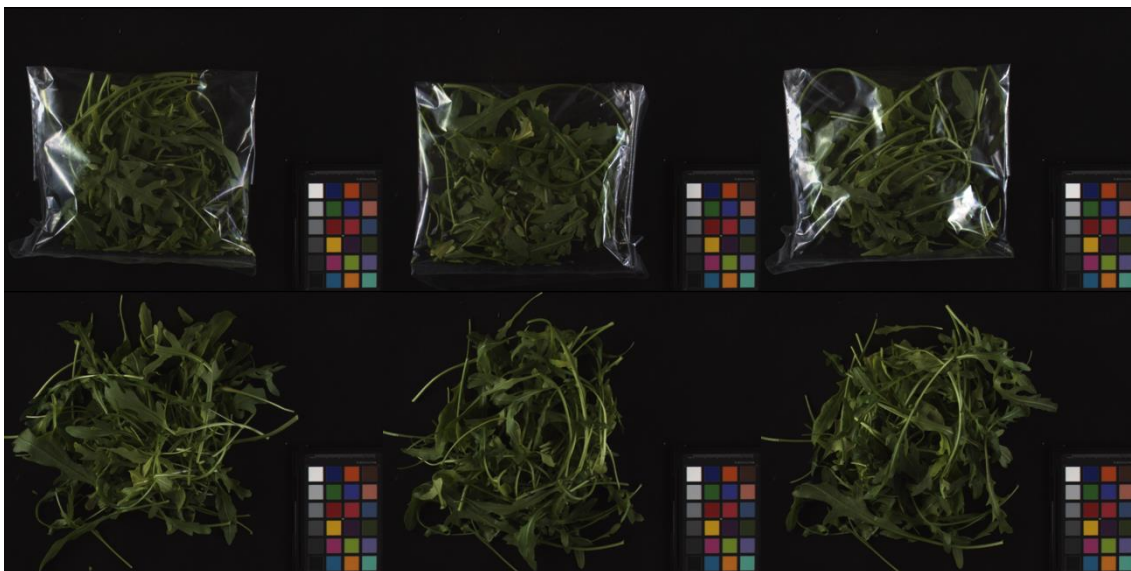
763

764 **Figure captions**

765 **Figure 1.** Example of the set of 6 images acquired for each sample. Three images were acquired with
766 the product inside a bag, shuffling the product between acquisitions. No care was given to the position
767 of the product in the bag nor to the position of the bag in the scene and to the highlights created by
768 the illumination on the surface of the bag. Then, the bag was open and three images of the same
769 product were acquired. The leaves were randomly shuffled and stacked before each acquisition. In all
770 the images a color-chart was placed in the scene to enable the color correction step needed to increase
771 the consistency of color evaluation.

772

773



774

775

776

777

778

779

780

781

THIS IS THE SUBMITTED VERSION.

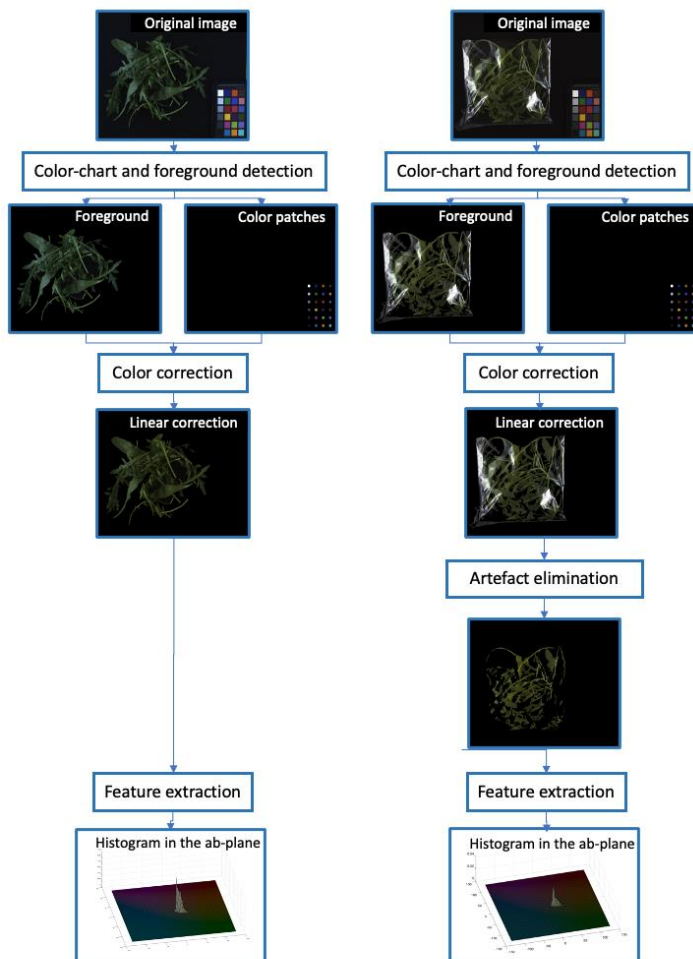
Published version: <https://doi.org/10.1016/j.postharvbio.2022.111910>

Palumbo, M., Pace, B., Cefola, M., Montesano, F. F., Colelli, G., & Attolico, G. (2022). Non-destructive and contactless estimation of chlorophyll and ammonia contents in packaged fresh-cut rocket leaves by a Computer Vision System. *Postharvest Biology and Technology*, 189, 111910.

782

783

784 **Figure 2.** The flow chart of the processing done on the images. It is possible to appreciate the effects
785 of each step on the image. The flowchart on the left is related to images of unpackaged products. The
786 flowchart on the right describes the processing of images of packaged products. The difference is
787 only in the artefact elimination step applied to packaged products: it is required to select the pixels
788 where meaningful colors can be measured by the camera. Data extracted from the patches of the color
789 chart was used to evaluate the parameters of the linear color correction model used. The final result
790 is a histogram of colors in the a-b plane of the CIE $L^*a^*b^*$ color space: the complete histogram is used
791 as feature vocabulary by the Random Forest classification and regression models used to assign the
792 visual quality to samples and to estimate their chlorophyll and ammonia contents.

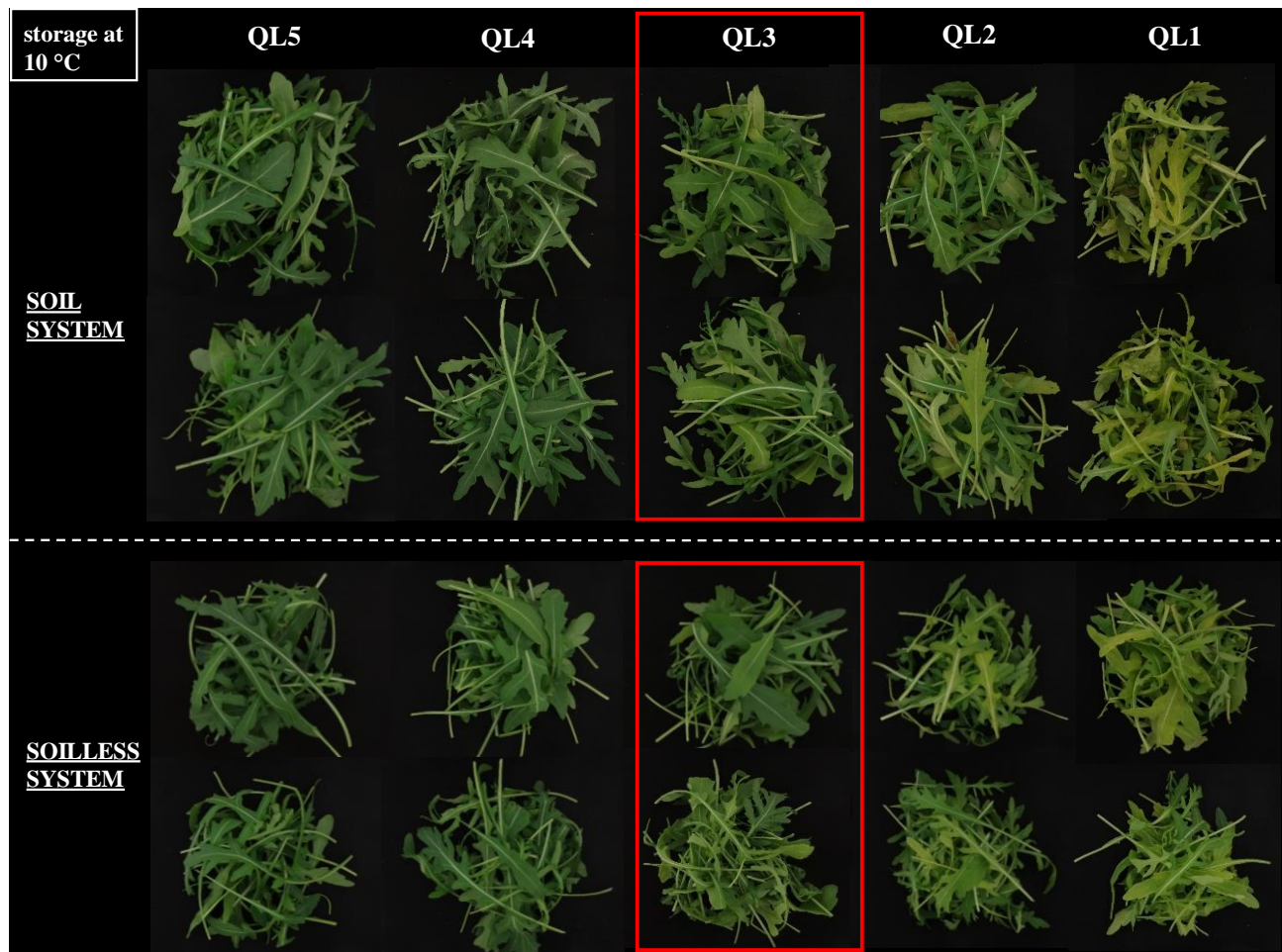


793

794

795 **Figure 3.** Changes in the sensory quality level (QL) of fresh-cut rocket leaves during the storage at
796 10 °C according to the 5 to 1 rating scale reported by Palumbo et al. (2021). In detail, QL5=very
797 good; QL4= good; QL3=fair; QL2=poor; QL1=very poor.

798



799

800

801

802

803

804

805

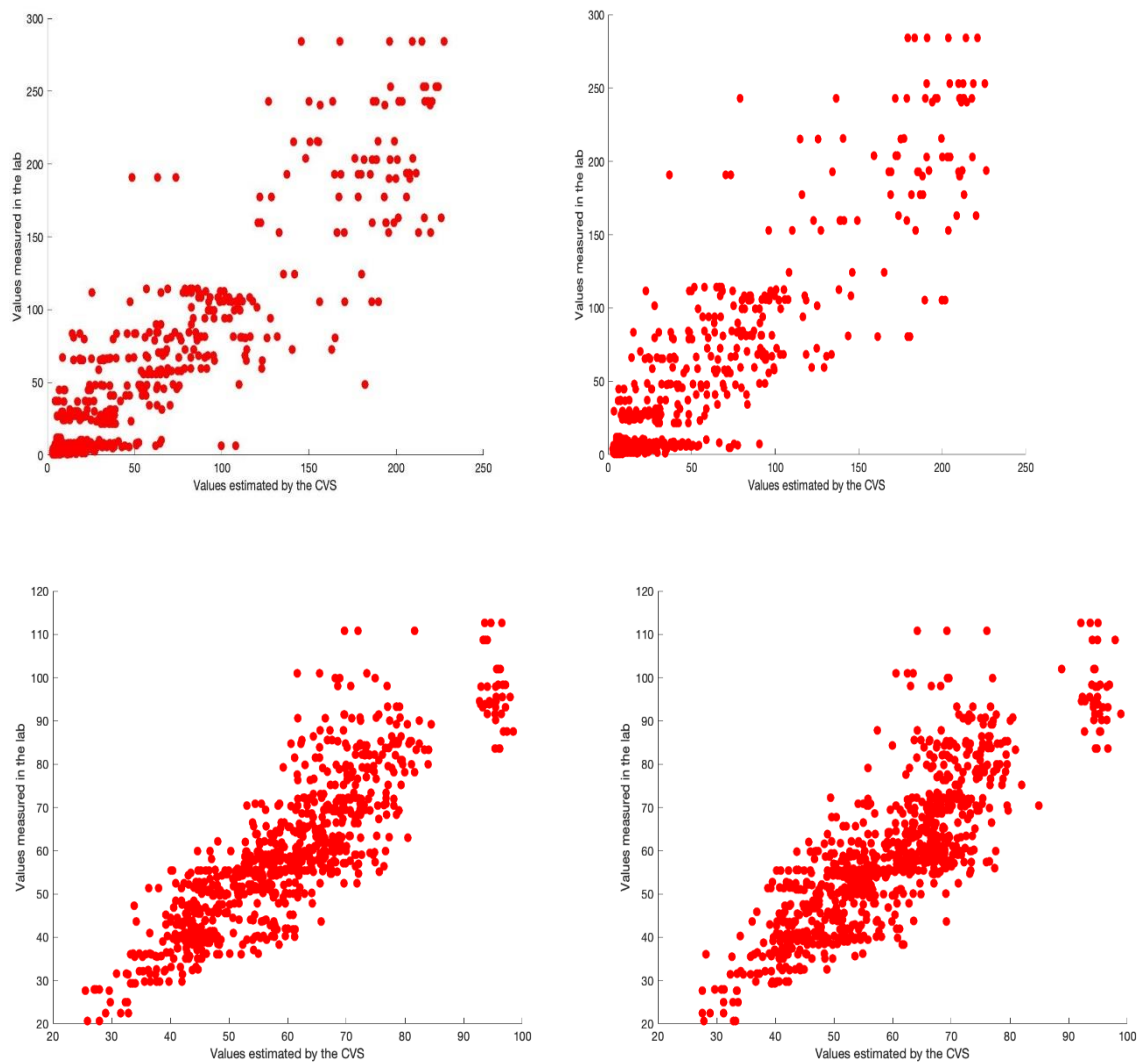
806

807 **Figure 4.** Values estimated by the CVS (abscissa) vs. values measured in the laboratory (ordinate)

808 for ammonia content on unpackaged (A) and packaged (B) rocket leaves and for total chlorophyll

809 content on unpackaged (C) and packaged (D) samples.

810



811

812

813

814

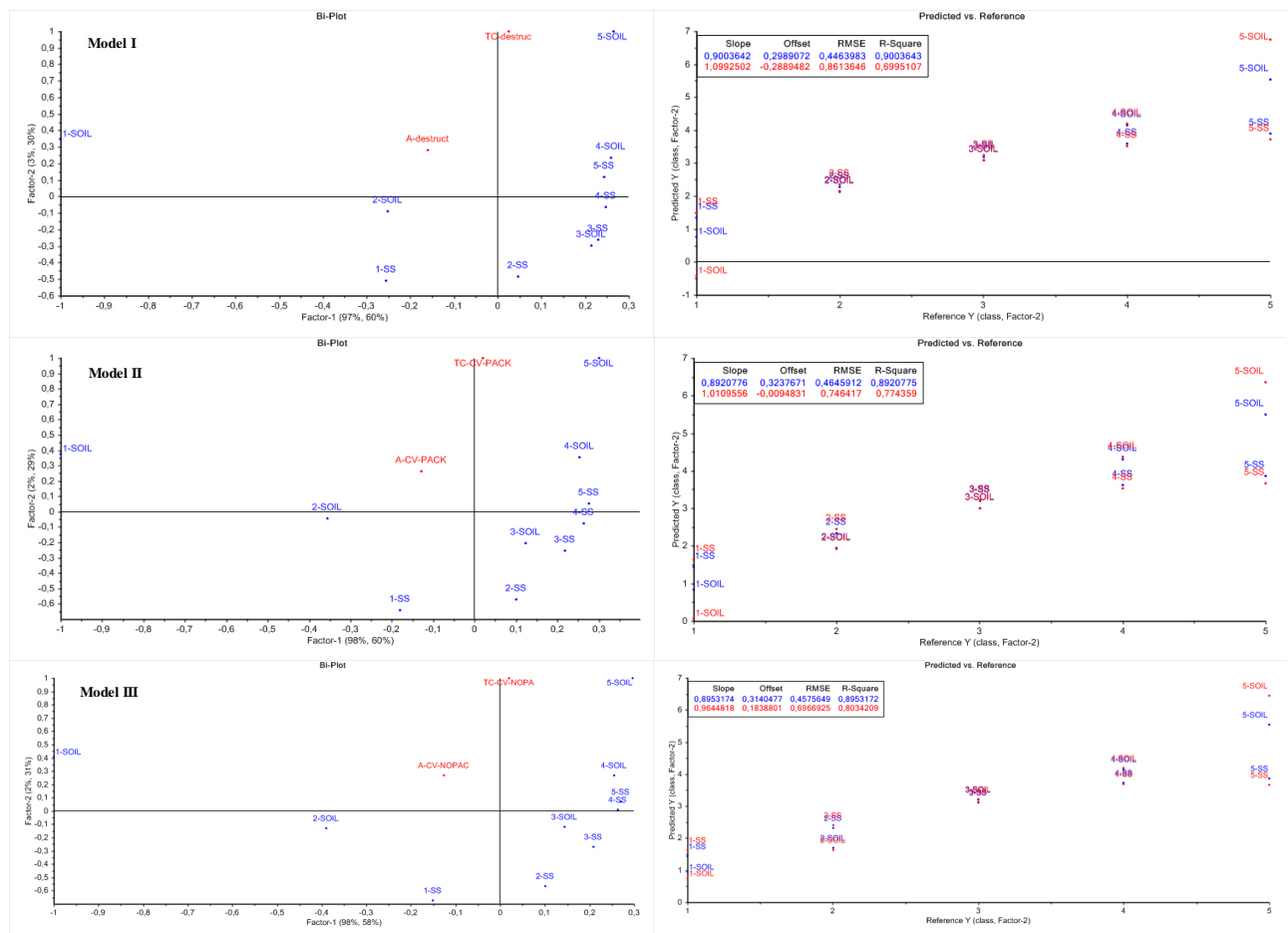
815

816

817

818 **Figure 5.** Models obtained by partial least squares regression (PLSR) to predict the sensory QL of
819 fresh-cut rocket leaves through total chlorophyll and ammonia contents. For each model, the biplot
820 and the comparison between predicted and reference for calibration (blue) and validation (red) step
821 are reported. In the first line, the chlorophyll and ammonia data come from the laboratory (Model I),

822 in the middle one, the same data are estimated by the CVS on packaged product (Model II). In the
 823 last line, the data are estimated by the CVS on unpackaged product (Model III). The graphics show
 824 the validity of chlorophyll and ammonia contents estimated by the CVS. Moreover, the observation
 825 through the packaging does not decrease significantly the effectiveness of the method.
 826



827